Synthesis of Thermoresponsive Mixed Arm Star Polymers by Combination of RAFT and ATRP from a Multifunctional Core and Its Self-Assembly in Water

Krishnan Ranganathan,[†] Rui Deng,[‡] Rajesh K. Kainthan,[†] Chi Wu,[‡] Donald E. Brooks,*[,†,§] and Jayachandran N. Kizhakkedathu*[,†]

Centre for Blood Research and Department of Pathology and Laboratory Medicine, University of British Columbia, Vancouver, BC V6T 1Z3, Canada; Department of Chemistry, The Chinese University of Hong Kong, Hong Kong; and Department of Chemistry, University of British Columbia, Vancouver, BC V6T 1Z3, Canada

Received January 14, 2008; Revised Manuscript Received April 21, 2008

ABSTRACT: Mixed arm star copolymers of poly(*N,N*-dimethylacrylamide) (PDMA) and poly(*N*-isopropylacrylamide) (PNIPAm) were synthesized by a sequential reversible addition−fragmentation chain transfer (RAFT) and atom transfer radical polymerization (ATRP) from a multi-initiator-functionalized hyperbranched polyglycerol (MI-HPG) core. The MI-HPG core was synthesized from an amine-functionalized polyglycerol, modified successively with 2-chloropropionamide groups (ATRP initiator) and 4,4′-azobis(4-cyanovaleric acid) (azo initiator). *N,N*-Dimethylacrylamide was polymerized from MI-HPG core by the RAFT method using *S,S*′-bis(α,α′-dimethyl-α″-acetic acid)trithiocarbonate as a chain transfer agent (CTA) in acetic acid/sodium acetate aqueous buffer solutions. The ratio of [CTA]/[azo initiator] was critical in controlling the molecular weight of the PDMA grafts from MI-HPG core (HPG-*g*-PDMA). Controlled synthesis of mixed arm star copolymers was achieved by cografting PNIPAm on to the HPG-*g*-PDMA macroinitiator by ATRP. The temperature-induced phase transition of aqueous solutions of hybrid HPG-*g*-PDMA/PNIPAm star copolymers was studied by ^{1}H NMR, UV−vis spectroscopy, and laser light scattering. Results show that the mixed arm star copolymers exist as either single molecules or small aggregates below the phase transition temperature (LCST) of PNIPAm in aqueous solutions. All the star copolymers formed intermolecular aggregates above the LCST of PNIPAm possibly due to the hydrophobic interaction between collapsed PNIPAM chains. These aggregates have micelle-like structure with PNIPAm core and PDMA corona. The formation of intermolecular aggregates and the stabilization of aggregates depend on the molecular weight of arms and composition of the star copolymer.

Introduction

Development of stimuli-responsive nanostructured materials including surface grafted polymers and self-assembled soluble polymers is a topic of current research interest.[1–4] Stimuli responsive water-soluble polymers have been widely investigated for potential applications in medicine, biotechnology, food, and cosmetics and as surfactants, additives for pharmaceutical formulations, and drug delivery vehicles.[5–7] Poly(*N*-isopropylacrylamide) (PNIPAm) has been the gold standard for these applications. Aqueous solution of PNIPAm and its copolymers undergo a reversible phase transition when stimulated by appropriate changes in temperature, pH, solvent, or in the presence of certain inorganic salts.[8] Apart from PNIPAm, other polymers such as N-substituted poly(acrylamide)'s,[9,10] poly(2-dialkylamino)ethyl methacrylates,[11–14] hydrophobically modified polyglycerols,[15,16] and copolymers of PEG[8,12–14] also exhibit similar phase transitions under appropriate external stimuli.[17,18]

Amphiphilic block copolymers and multiarm star polymers can self-assemble to form micelles or reverse micelles in aqueous solution, depending on external conditions such as temperature, pH, and ionic strength.[19–43] Block copolymer micelles usually have a large aggregation number, and their self-assembly is not stable as shown by the existence of dynamic exchange between micelles and unimers. They tend to be destroyed by shear forces, dilution, or salinity.[7,44] An alternate and facile approach is to develop the so-called "unimolecular micelles" and amphiphiles that are tethered to a multifunctional core.[41–43,45–47] Examples are heteroarm star copolymer and dendritic macromolecules for which the formation of "unimolecular micelles" has been demonstrated.[41–43,45–47] Compared to conventional block copolymer micelles, such assemblies offer much higher stability in aqueous solution due to covalent attachment of individual components of the assembly to the same core.

Controlled radical polymerizations such as atom transfer radical polymerization (ATRP) and reversible addition−fragmentation chain transfer (RAFT) methods have been used to produce polymers with well-defined structures, predictable molecular weights, and end groups with narrow molecular weight distributions.[48–52] Although the combination of RAFT and ATRP has been previously used for the synthesis of graft copolymers,[53] the polymerization from multifunctional initiator core using sequential ATRP and RAFT is relatively new. The advantage here is that one can benefits from both types of controlled polymerization techniques for the creation of well-defined structures with tunable properties. While we were preparing this manuscript, Liu et al. have published on the use of a combination strategy in the development mixed star copolymers of polystyrene and poly(*t*-Bu acrylate) on a hyperbranched polyglycerol core.[40]

Our goal from this research is to create stimuli responsive mixed arm star copolymers containing both stimuli responsive arms and nonresponsive arms whose properties can be controlled. Such copolymers could potentially form stable core−shell assemblies in aqueous solution without precipitation above the phase transition of stimuli responsive arms. To achieve this,

* To whom correspondence should be addressed: e-mail jay@pathology.ubc.ca (J.N.K.), Ph 604-822-7085, Fax 604-822-7742; e-mail don.brooks@ubc.ca (D.E.B.).
[†] Centre for Blood Research, University of British Columbia.
[‡] The Chinese University of Hong Kong.
[§] Department of Chemistry, University of British Columbia.

10.1021/ma800094d CCC: $40.75
Published on Web 05/24/2008

co-grafted poly(*N*,*N*-dimethylacrylamide) (PDMA) and poly(*N*-isopropylacrylamide) (PNIPAm) were grown from a multi-initiator-functionalized core made from a low molecular weight hyperbranched polyglycerol by sequential RAFT and ATRP polymerizations. We have investigated the aggregation behavior of these mixed arm star polymers to understand the conditions at which these copolymers form stable and soluble nanostructures.

Experimental Section

Materials. All commercial reagents were purchased from Aldrich (Oakville, ON) and used without further purification unless otherwise noted. *N*,*N*-Dimethylacrylamide (DMA, Aldrich, 99%) was purified by vacuum distillation and stored at −20 °C until use. *N*-Isopropylacrylamide (NIPAm) was recrystallized using a hexane: toluene (65:35 v/v) mixture and stored at 4 °C until use. 1,1,4,7,10,10-Hexamethyltriethylenetetramine (HMTETA, Aldrich, 97%) and tris[2-(dimethylamino)ethyl]amine (Me_6TREN), prepared following a reported procedure[54] from tris(2-aminoethyl)amine (TREN) (Aldrich, 96%), were used as ligands for ATRP. The chain transfer agent *S*,*S*′-bis(α,α′-dimethyl-α″-acetic acid)trithiocarbonate was synthesized following a reported procedure.[55]

Methods. ^{1}H NMR spectra were recorded on a Bruker Avance 300 MHz NMR spectrometer using DMSO-d_6 or D_2O (Cambridge Isotope Laboratories) with the solvent peak as a reference. Monomer conversion was determined by reverse-phase HPLC analysis on a Hitachi model L-6210 HPLC fitted with a L-4200 UV−vis detector and a Lichrospher 60 RP-select B reverse phase column from Merck at $\lambda = 236$ nm using aqueous 0.1% trifluoroacetic acid (TFA) solution as the mobile phase at a flow rate of 4 mL/min at 22 °C. Absolute molecular weights and molecular weight distributions of the polymers were determined by gel permeation chromatography (GPC) on a Waters 2695 separation module fitted with a DAWN EOS multiangle laser light scattering (MALLS) detector (laser wavelength $\lambda = 690$ nm) and an OPTILAB refractive index detector operated at $\lambda = 620$ nm from Wyatt Technology Corp. Aqueous 0.1 M $NaNO_3$ solution was used as the mobile phase at a flow rate of 0.8 mL/min. The d*n*/d*c* of the copolymers were calculated using the equation

$$(dn/dc)_{hybrid} = (WF)_{PDMA}(dn/dc)_{PDMA} + (WF)_{PNIPAm}(dn/dc)_{PNIPAm}$$

where WF is the weight fraction. We used 0.150 and 0.164 as the d*n*/d*c* of PDMA and PNIPAm homopolymers, respectively, in 0.1 M $NaNO_3$ solution as reported previously.[56] Turbidity measurements of aqueous solution of polymers were made with a UV−vis spectrophotometer (CARY 4000) equipped with a temperature controller. Measurements were made at 500 nm with a heating rate of 0.5 °C/min at a polymer concentration of 1 mg/mL.

Synthesis of a Multi-Initiator-Functionalized HPG Core (MI-HPG). Multifunctional initiators containing both ATRP and azo initiators were synthesized from an amine-functionalized hyperbranched polyglycerol (HPG-amine) core in a two-step procedure. The hyperbranched polyglycerol core was synthesized by a ring-opening multibranching anionic polymerization as reported.[57] Appproximately 20 hydroxyl groups of HPG ($M_n = 3000$, PDI = 1.20; total number of hydroxyl groups ∼40) were first converted to tosylate by a reaction with tosyl chloride.[59] The tosylate groups were then converted to amine groups by reacting with tris(2-aminoethyl)amine (TREN) in dioxane at 100 °C.[58,59] ^{1}H NMR quantitation showed the presence of ∼40 NH_2 groups per molecule. This step generated 2 primary amine groups/TREN reacted. ^{1}H NMR (DMSO-d_6, 300 MHz): $\delta = 2.45$ (t, CH_2), 2.55 (t, CH_2), 3.05 (s, NH and NH_2), 3−4 (m, PG).

a. Incorporation of ATRP Initiators on HPG Core (HPG-ATRP). The ATRP initiators, 2-chloropropionamide group, were introduced into the HPG-amine core (3 g) by reaction of primary amine groups with 2-chloropropionyl chloride (1.2 g, ∼40% conversion of amine groups) in the presence of triethylamine (1.25 mL) in chloroform: methanol (5:95) solvent mixture. HPG-amine and triethylamine were dissolved in 50 mL of methanol in a round-bottom flask and cooled in an ice bath. 2-Chloropropionyl chloride dissolved in 2.5 mL of chloroform was added dropwise to this mixture over a period of 1 h and stirred at 0 °C for another 8 h. The solvent was removed by rotary evaporator, and the product was precipitated twice from acetone and dried in vacuum. ^{1}H NMR (DMSO-d_6, 300 MHz): $\delta = 1.5-1.6$ ppm (CH_3, ATRP initiator), 2.4 ppm ($-CH_2-$, from TREN), 3.4−4.00 ppm (from PG backbone).

b. Incorporation of Azo Initiators. The multifunctional initiator (MI-HPG) was synthesized by a reaction of the remaining primary amine groups of HPG-ATRP with 4,4′-azobis(4-cyanovaleric acid) using *N*,*N*-dicyclohexylcarbodiimide as a catalyst. The HPG-ATRP initiator (3.0 g) and 4,4′-azobis(4-cyanovaleric acid) (1.5 g) were dissolved in methanol:chloroform mixture (25:75), and then *N*,*N*-dicyclohexylcarbodiimide (2.5 g) was added and stirred for 2 days at room temperature. The solvent was removed by rotary evaporation at low temperature (below 30 °C), and product was precipitated in cold acetone and vacuum-dried. The amount of azo and ATRP initiators incorporated into the HPG-amine core was determined by ^{1}H NMR from the peaks corresponding to the polyglycerol core and methyl protons of ATRP initiator (1.5−1.6 ppm) and azo initiator (1.6−1.7 ppm). ^{1}H NMR (DMSO-d_6, 300 MHz): $\delta = 1.5-1.6$ ppm (CH_3 ATRP initiator), $\delta = 1.6-1.7$ ppm (2 CH_3 azo initiator), $\delta = 2.2-2.4$ ppm ($-CH_2-CH_2-C-$, azo group), $\delta = 3-4$ ppm (b, PG backbone, from CH_2- near amide group).

Synthesis of Mixed Arm Star Copolymers. The star copolymers containing PDMA and PNIPAm were synthesized from the MI-HPG core by a two-step procedure.

a. Synthesis of HPG-g-PDMA by RAFT Method. In a typical RAFT polymerization experiment, a glass tube was charged with MI-HPG initiator (10 mg, azo initiator content ∼30 μmol), *N*,*N*-dimethylacrylamide (DMA) (2 mL, 19.4 mmol), *S*,*S*′-bis(α,α′-dimethyl-α″-acetic acid)trithiocarbonate (CTA) (8.4 mg, 0.029 mmol), and acetic acid/sodium acetate buffer (4 mL). The buffer solution and monomer were purged with argon and transferred to a glovebox under an argon atmosphere. The glass tube was heated at 70 °C in a preset oil bath for 20 h. The glass tube was taken out of the glovebox, and monomer conversion was determined by HPLC measurements by injecting the diluted polymerization solution. The monomer conversion was calculated using a calibration curve produced from known concentrations of DMA. The RAFT synthesized HPG-*g*-PDMA was diluted with water, excess 4,4′-azobis(4-cyanovaleric acid) was added to the solution in a ratio of 1:30 times relative to [CTA], and the solution was purged with argon and stirred at 80 °C for 24 h to remove incorporated CTA on the polymer chain end. After the reaction, the polymer was dialyzed against water for 1 week using a membrane with a MWCO of 10 000 to remove the low molecular weight impurities and cleaved chain transfer agent. The polymers were recovered by lyophilization. The absolute molecular weight and molecular distribution of the polymers were determined by GPC-MALLS using the d*n*/d*c* of PDMA since the weight fraction of the HPG core was negligible (<0.04 wt %). Different experiments were carried out by changing the concentration of chain transfer agent, initiator, and solvent conditions. To test the purity of the final HPG-*g*-PDMA macroinitiators, selected samples were further dialyzed with 25 000 and 50 000 MWCO cellulose membranes for 3 days, and molecular weight and molecular weight distribution are analyzed and compared using GPC-MALLS (Figures 1S−9S and Table 1S, Supporting Information).

b. Synthesis of HPG-g-PDMA/PNIPAm by ATRP. HPG-*g*-PDMA polymers were used as ATRP macroinitiators for the polymerization of *N*-isopropylacrylamide. In a typical ATRP polymerization, 250 mg of HPG-*g*-PDMA core containing ATRP initiator, Cu(I)Cl (10 mg, 0.1 mmol), Me_6TREN (22.5 mg, 0.1 mmol), NIPAm (1 g, 8.83 mmol), and water (3 mL) were used. The solvent water was degassed separately and transferred to a glovebox. The aqueous solution of HPG-*g*-PDMA initiator, monomer, Cu(I)Cl, and Me_6TREN was added, and the polymerization was carried out at room temperature (22 °C) for 24 h. The final star copolymers were purified by dialysis using a membrane (MWCO 10 000 Da) against water and lyophilized. The molecular weight, molecular weight

Scheme 1. Synthetic Routes for the Development of ATRP and Azo Initiator Functionalized HPG Core: (a) Tosylation with *p*-Toluenesulfonyl Chloride, (b) Amination with Tris(2-aminoethyl)amine (TREN), (c) Incorporation of ATRP Initiator, and (d) Incorporation of Azo Initiator

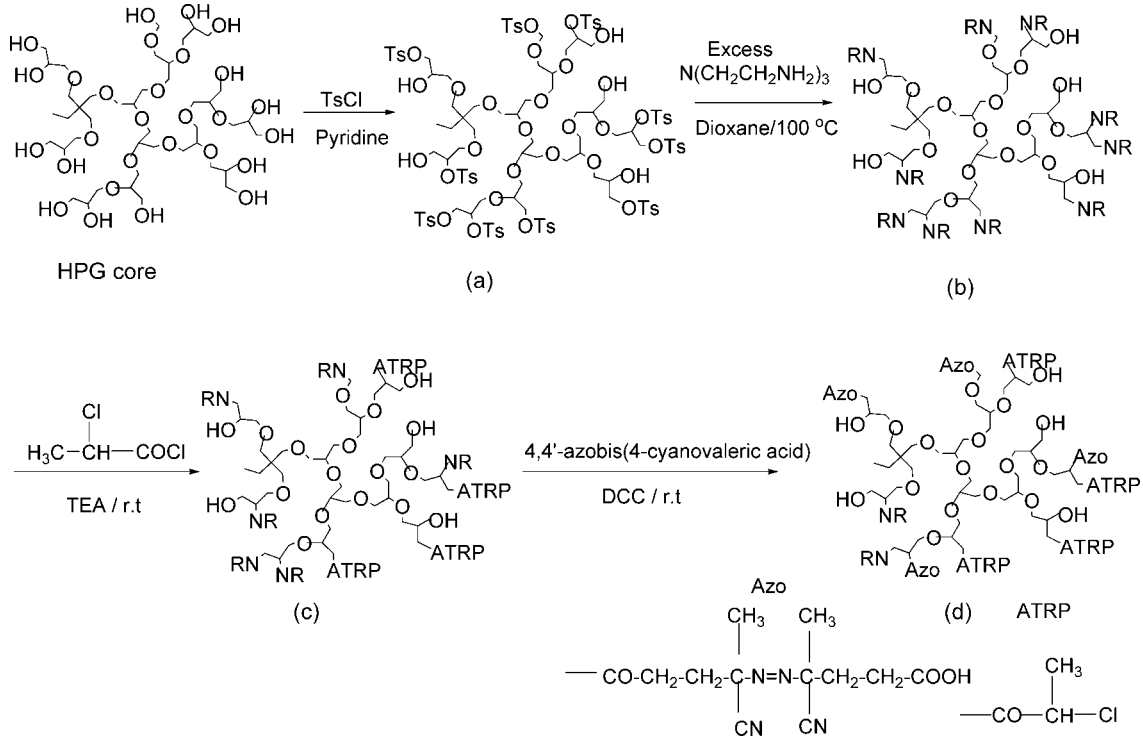

distribution, and composition of the copolymers were determined by GPC-MALLS and ^{1}H NMR analysis. Different experiments were carried out by changing the catalyst concentration, monomer concentration, and molecular weight of macroinitiators.

LCST Measurements. The LCSTs of the star copolymer solutions at 0.1 wt % were measured as a function of temperature at $\lambda = 500$ nm at a heating/cooling rate of 0.5 °C/min.

Laser Light Scattering (LLS) Measurements. A commercial LLS instrument (ALV5000) with a vertically polarized 22 mW He−Ne laser head (632.8 nm, Uniphase) was used. In static LLS (SLS), the scattering vector (q) dependence of the absolute excess time-averaged scattered intensity, known as the Rayleigh ratio $R_{vv}(q)$, can be related to the weight-average molar mass (M_w) and the z-average root-mean-square radius of gyration ($\langle R_g^2\rangle_z^{1/2}$ or $\langle R_g\rangle$) of the scattering objects and the second virial coefficient (A_2) of the dispersion or solution by

$$\frac{KC}{R_{vv}(q)} \cong \frac{1}{M_w}\left(1 + \langle R_g^2\rangle q^2\right) + 2A_2C \qquad (1)$$

where $K = 4\pi^2 n^2 (dn/dC)^2/(N_A\lambda_0^4)$ and $q = (4\pi n/\lambda_0)\sin(\theta/2)$ is the scattering vector with N_A, dn/dC, n, λ_0, and θ being Avogadro's number, the specific refractive index increment, the refractive index of solvent, the wavelength of the light in vacuum, and the scattering angle, respectively.

In dynamic LLS (DLS), the Laplace inversion of each measured intensity−intensity time correlation function $G^{(2)}(q,t)$ in the self-beating mode can be related to a line-width distribution $G^{(2)}$. For a diffusive relaxation, Γ is related to the translational diffusion coefficient D by $(\Gamma/q^2)_{C\to 0,q\to 0}) = D$, so that $G(\Gamma)$ can be converted into a transitional diffusion coefficient distribution $G(D)$ or a hydrodynamic radius distribution $f(R_h)$ via the Stokes−Einstein equation, $R_h = (k_BT/6\pi\eta)D^{-1}$, where k_B, T, and η are the Boltzmann constant, the absolute temperature, and the solvent viscosity, respectively.

All the samples were dissolved in appropriate amount of deionized water at two concentrations (0.5 and 0.0625 mg/mL) and passed through a 100 nm filter. DLS and SLS measurements were carried out at 25, 30, 32, 34, 36, 40, and 50 °C for each sample. The polymer solutions were allowed to thermally equilibrate for ca. 30 min to obtain stable scattering intensity before the measurements were taken.

Results and Discussion

Hydrolytically stable multifunctional core containing both free radical initiator and ATRP initiator was synthesized by a two-step procedure (Scheme 1). A hyperbranched polyglycerol having a degree of polymerization of 40 with narrow molecular weight distribution ($M_w/M_n = 1.2$) was used. Primary amine functionalities were introduced after conversion of the hydroxyl groups to tosylates followed by reaction with TREN. The HPG-amine had ~40 primary amine groups per molecule as determined by ^{1}H NMR. We have modified ~16 amine groups each with 2-chloropropionamide group and with 4,4′-azobis(4-cyanovaleric acid). This MI-HPG macroinitiator was used for the synthesis of mixed arm star copolymers containing thermoresponsive PNIPAm and a highly water-soluble PDMA cografted on the hyperbranched core.

An idealized structure is shown in Figure 1. These mixed arm star copolymers are expected to form core−corona structures with PNIPAm/HPG core and PDMA corona above the LCST of the PNIPAm under appropriate conditions. The formation of such core−shell structures depends on the composition and molecular weight of each component in the final star copolymer. The key to achieving this was the development of a controlled RAFT and ATRP method from the multi-initiator-functionalized core. We have used a two-step polymerization procedure, RAFT polymerization of DMA from MI-HPG macroinitiator and ATRP of NIPAm from the HPG-*g*-PDMA macroinitiator, to synthesize the final cografted mixed arm star copolymer.

RAFT Polymerization of *N,N*-Dimethylacrylamide. RAFT polymerization[51] and macromolecular design by interchange of xanthates[60] are the most versatile techniques in aqueous controlled radical polymerization of (meth)acrylamides and

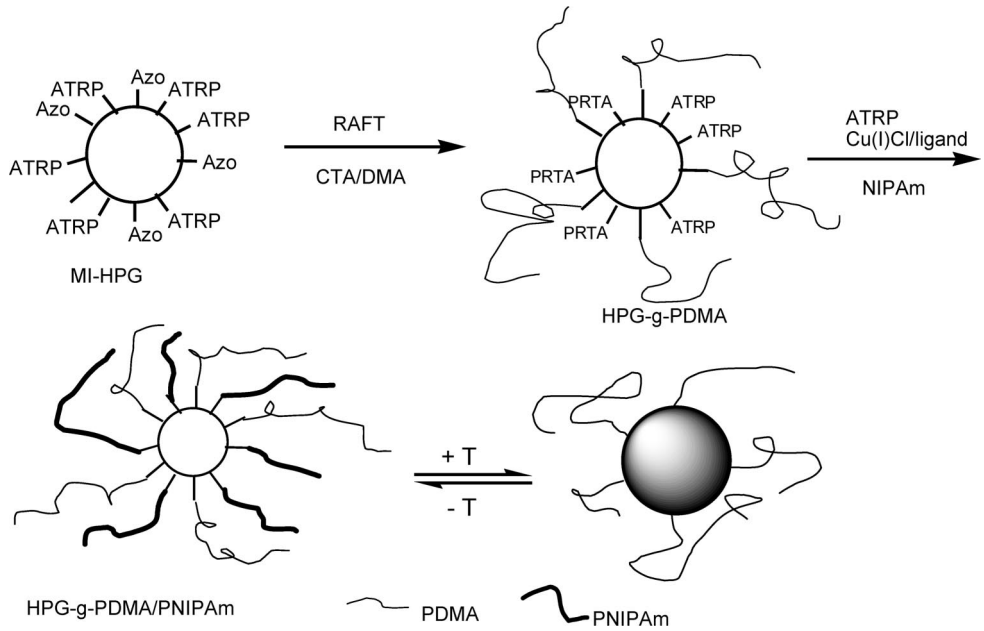

Figure 1. Schematic representation of the synthesis of hybrid copolymers of HPG-*g*-PDMA/PNIPAm synthesized from MI-HPG core by combination of RAFT and ATRP techniques. An idealized structure for the formation of particles with core−corona structure is also given.

Table 1. Monomer Conversion, Molar Mass (M_n), and Polydispersity (M_w/M_n) Data for HPG-*g*-PDMA Polymers Synthesized by RAFT Polymerization of *N,N*-Dimethylacrylamide at 70 °C from MI-HPG Core[a]

initiator (mg)	[CTA]/[I]	DMA (mL)	solvent	% conv	$M_{n,th}$[b]	$M_{n,GPC}$	M_w/M_n	mol wt of individual arms[c]
25	5	2	DMSO					
25	1	2	DMSO	48	15 500	21 400	1.24	700
10	2	2	buffer	95	34 000	58 500	1.20	2900
10	1	2	buffer	95	62 000	75 000	1.17	3900
10	0.5	2	buffer	98	131 000	129 000	1.23	7300
10	0.25	2	buffer	98	245 000	244 000	1.26	14500

[a] Experimental conditions: azo initiator concentration = 3.0×10^{-3} mol/g, buffer = acetic acid/sodium acetate buffer solution (pH = 5.2), reaction time = 20 h. CTA: *S,S*′-bis(α,α′-dimethyl-α″-acetic acid)trithiocarbonate, volume = 4 mL. [b] $M_{n,th} = \{[M]_0/[CTA]_0 \times M_{w,DMA} \times c\} + M_{n,initiator}$; $M_{n,initiator}$ is the molecular weight of MI-HPG. [c] Theoretical molecular weight assuming 100% initiator efficiency.

(meth)acrylic acid monomers.[52,53] These methods allow the synthesis polymers with predetermined molecular weights, low polydispersity, different architectures, and compositions from a wide range of vinyl monomers.[52,53]

Several experimental conditions were investigated for synthesizing the HPG-*g*-PDMA copolymer by RAFT; the results are given in Table 1. Initial RAFT polymerization of DMA from the MI-HPG core was conducted using *S,S*′-bis(α,α′-dimethyl-α″-acetic acid)trithiocarbonate as chain transfer agent and DMSO as solvent at [CTA]/[I] = 5. No polymerization was observed in this case. Upon decreasing [CTA]/[I] ratio, DMA was polymerized from MI-HPG core, and the molecular weight of the resulting polymer was M_n 21 400 (Table 1, entry 2). But the molecular weight and conversion were low in this case. Reactions in DMSO were not successful possibly due to the low solubility of *S,S*′-bis(α,α′-dimethyl-α″-acetic acid)trithiocarbonate (CTA) in DMSO, which was shown to influence the RAFT polymerization.[61] In a related study McCormick et al. demonstrated that the addition of organic solvents like DMF could influence the polymerization kinetics in aqueous RAFT polymerization of DMA.[62] The fragmentation of chain transfer agents can also be influenced by the nature of the solvents.[62] The solubility of the grafted PDMA on MI-HPG core in DMSO may be another factor influencing the polymerization in our case. Because of these reasons, we have changed the polymerization medium to an acidic buffer for further experiments. We used acetic acid/sodium acetate buffer at pH ∼ 5.2, as chain transfer agents are highly susceptible to hydrolysis in water above pH ∼ 6.0.[63,64] For RAFT polymerization in these conditions, conversions were high, and we obtained narrowly distributed HPG-*g*-PDMA polymers (Table 1, entries 3−6). The enhanced solubility of both our CTA and PDMA in water might have resulted in an increased polymerization rate and high conversions. The molecular weight of the polymers increased with decreasing [CTA]/[I] ratio with high molecular weight (M_n 244 000) obtained at a ratio of 0.25 at constant monomer concentration. The increase in molecular weight with decrease in the [CTA]/[I] is consistent with reported literature.[62] $M_{n,GPC}$ values of HPG-*g*-PDMA copolymers were slightly higher than $M_{n,th}$ values, and narrow polydispersities were observed. Slight increase in the polydispersity of polymers (1.17 to 1.26) with decrease in the CTA concentration with respect to initiator (from 2 to 0.25) may be due to the lose of active chain transfer agent by aminolysis. The residual primary amine groups on the initiator may react with the chain transfer agent. This is more relevant when there is less amount of CTA compared to initiator. We could not avoid the presence of residual primary amine groups as it was necessary for the solubility of multifunctional initiator in water.

Since the individual PDMA arms were connected to the HPG core through hydrolytically stable amide bonds, the individual chains could not be cleaved from the core. So, we estimated the molecular weight of the PDMA arms (theoretical) based on the final molecular weight of the HPG-*g*-PDMA star polymer and number of initiators present. The arms length varied from 700 to 14 500 Da. We assumed a 100% initiator efficiency in this case. But the actual values of individual arms length may be different than these values due to the low initiator efficiency in the case of multi-initiator systems. Typical values reported in the literature were in the range 5−93%.[40,65] Also, the numbers

Table 2. Molar Mass (M_n), Polydispersity (M_w/M_n), and Composition of HPG-*g*-PDMA/PNIPAm Star Copolymers Synthesized by ATRP of NIPAm at Room Temperature from HPG-*g*-PDMA Core[a]

	catalyst system	HPG-*g*-PDMA ATRP macroinitiator M_n	Cu(I)Cl (mmol)	NIPAm (g)	copolymer $M_{n,GPC}$ (M_w/M_n)	M_n of PNIPAm arms[b]	composition from ^{1}H NMR PDMA:PNIPAm	mol wt of PNIPAm arms from ^{1}H NMR composition[c]
C1	Me_6TREN	75 000 (250)	0.03	1	77 500 (1.20)	156	85.5:14.5	860
C2	Me_6TREN	75 000 (250)	0.07	1	80 000 (1.22)	312	88.7:11.3	640
C3	Me_6TREN	75 000 (250)	0.11	1	104 000 (1.34)	1800	70.3:29.7	2140
C4	Me_6TREN/Cu(II)Cl_2	129 000 (100)	0.042	0.4	247 000 (1.39)	7400	33.7:66.3	17600
C5	Me_6TREN/Cu(II)Cl_2	244 000 (100)	0.050	0.4	400 000 (1.62)	9700	36.3:63.7	30270
C6	Me_6TREN/Cu(II)Cl_2	129 000 (100)	0.042	0.6	426 000 (1.95)	18 500	32.5:67.5	18500
C7	HMTETA/Cu(II)Cl_2	129 000 (100)	0.043	0.4	136 000 (1.56)	437	83.4:16.6	1780

[a] Experimental conditions: reaction time = 20 h, Cu(I)Cl:ligand = 1:1, Cu(II)Cl_2 = 15 mol % to Cu(I)Cl, solvent = water (3 mL). [b] Theoretical molecular weight assuming 100% initiator efficiency. [c] Theoretical molecular weight calculated from ^{1}H NMR molar composition assuming 100% initiator efficiency. Absolute molecular weight of HPG-*g*-PDMA is taken as standard for this calculation.

of initiators on MI-HPG core reported are average numbers due to the polymeric nature of our macroinitiator.

The incorporated CTA on PDMA chain ends was removed by reaction with excess azo initiator. This step eliminates the possible side reaction of PDMA-anchored CTA with free radicals in the next step, growing PNIPAm chains from HPG-*g*-PDMA by ATRP.[66] To verify the purity of the HPG-*g*-PDMA macroinitiators, selected samples were further dialyzed with 25 and 50 kDa cellulose membranes. The molecular weight and molecular weight distribution of the dialyzed samples were determined by GPC-MALLS and compared with the original samples (Figures 1S−9S and Table 1S in the Supporting Information). The analysis showed that there is no significant change in the molecular weight or molecular weight distribution indicating the absence of any low molecular weight fractions in the samples. The absence of high molecular weight species in LS chromatogram (see Figures 3S, 6S, and 9S) rules out the possibility of bimolecular termination and star−star coupling during the polymerization. Also, the low polydispersity of the HPG-*g*-PDMA macroinitiators is indicative of the absence of termination within the molecules and any unwanted side reactions between CTA and ATRP initiator groups, which is consistent with other reports in the literature.[53] The measured zeta potential of the star copolymers at different pH (4, 7, 9) indicates that they do not have a sufficient number of anionic charges present to make them pH sensitive.

Atom Transfer Radical Polymerization of *N*-Isopropylacrylamide. We used three HPG-*g*-PDMA macroinitiators (HPG-*g*-PDMA-75K, -129K, and -244K) for these experiments. Our working hypothesis was that a longer non-thermoresponsive PDMA chains attached on a core should stabilize the shorter thermoresponsive PNIPAm chains cografted on to the same core above its LCST to form stable core−shell assemblies. Such assemblies could potentially form "unimolecular micelles" depending on the composition and molecular weight of HPG-*g*-PDMA/PNIPAm star polymer. We experimented with different catalyst and monomer concentrations to obtain polymers having different composition and molecular weight. ATRP of NIPAm was initiated from 2-chloropropioamido initiators on the HPG-*g*-PDMA core at room temperature to form a co-grafted mixed arm star polymeric structure as shown in Figure 1.

Initial experiments in isopropanol:water (75:25) mixture using Me_6TREN/Cu(I)Cl catalyst produced a bimodal distribution of molecular weights with low conversion (data not shown), suggesting ineffective initiation in these experiments compared to homopolymerization of NIPAm in an alcoholic medium.[18] Changing the polymerization medium to water gave better results as shown in Table 2. For a given macroinitiator molecular weight and monomer concentration, the molecular weight of the arms increased with increase in catalyst concentration (Table 2, C1 to C3). The amount of catalyst present may not be sufficient to produce successful growth of larger PNIPAM arms from macroinitiators at low catalyst concentrations. This may be due to the fact that the exact concentration of ATRP initiators present in the reaction medium was difficult to calculate owing to the high molecular weight and polydispersity of HPG-*g*-PDMA macroinitiators. The accessibility catalysts to initiator groups (ATRP is a bimolecular process) may be another factor governing the polymerization; in the present case initiator groups are protected by soluble PDMA chains. Similar observations were reported by Frey et al. in a recent report on the synthesis of star polymers from hyperbranched core by ATRP.[67]

All the mixed star copolymers had unimodal distributions of molecular weights as seen from the GPC traces (see Figures 10S−17S; Supporting Information). The polydispersity of the HPG-*g*-PDMA/PNIPAm mixed arm star polymer was higher than the macroinitiators and increased with increase in monomer concentration and molecular weight of macroinitiators. The increase in the polydispersity of mixed star polymers may be due to the coupling reactions between the radicals at high conversions such as in our case. Similar observations were previously reported for other star polymer systems.[68] The probability of such side reactions in the present case may be lower due to the possible SET-LRP mechanism (active species is Cu(0)) during the polymerization using Me_6TREN/CuCl catalyst in water[69] instead of true ATRP. Percec et al. have previously reported the successful synthesis of an 8-arm star polymer with molecular weights up to 1 000 000 Da in polar solvents at high conversions (~85%) using this method.[69a] They did not observe any cross-coupling between the star molecules even at high conversions.

The most probable reason for the increase in polydispersity is the inefficient initiation from high molecular weight HPG-*g*-PDMA initiators (Table 2, entries C4−C6) due to the steric hindrance from existing polymer chains on HPG-*g*-PDMA macroinitiator. Very recently, Liu et al. have reported a similar observation that an increase molecular weight of macroinitiator decreased the initiator efficiency and increased the polydispersity of the final star polymer.[40] Although the mixed arm star polymers did not produce a significant difference in the retention volume in GPC measurements, the cumulative weight fraction and absolute molecular weight of polymers determined by static light scattering (Figures 10S−17S; Supporting Information) show there is a clear separation between the HPG-*g*-PDMA macroinitiator and resulting HPG-*g*-PDMA/PNIPAm star polymer. These results were also supported by the composition analysis by ^{1}H NMR (Table 2). With increase in molecular weight of the HPG-*g*-PDMA/PNIPAm mixed arm star polymer there is a corresponding increase in its PNIPAm content. The composition obtained from ^{1}H NMR is higher than that calculated from M_n obtained; the difference may be due to the higher molecular weight distribution of the polymers (Table 2).

Since the individual PNIPAm arms are attached to HPG core through hydrolytically stable amide bonds, it was difficult to analyze the individual molecular weight of the arms. For the same reasons, the initiator efficiency was difficult to determine. Theoretical molecular weights of the PNIPAM arms are given in Table 2. Also given are the molecular weights of the PNIPAm arms calculated from the ^{1}H NMR composition data.

The molecular weights and the composition of the star copolymers were varied using different macroinitiators and monomer concentrations. When using the same macroinitiator (HPG-*g*-PDMA (129K), an increase in monomer concentration resulted in an increase in the molecular weight of the PNIPAm grafts (Table 2, entries C4 and C6). This is due to the fact that at constant initiator concentration an increase in the amount of monomer would result an increase in molecular weight. The catalyst concentration (Table 2, entries C1−C3), use of $Cu(II)Cl_2$ along with Cu(I)Cl (entries C4−C7), and use of different catalyst (Me_6TREN/CuCl vs HMTETA/CuCl) have different effects on the molecular weight and composition of hybrid copolymers. The effect on molecular weight with increase in catalyst concentration (entries C1−C3) could be due to the increase rate of polymerization with the addition of active Cu(I) species at constant monomer concentration and also efficient initiation from the macroinitiators. It has been reported previously that the rate of polymerization increases with increase in catalyst concentration.[70] The observed difference in molecular weight of mixed star polymer with different catalyst systems Me_6TREN/CuCl vs HMTETA/CuCl is be due to the difference in the reactivity of these catalysts due to the slow activation and fast deactivation of linear amine catalyst.[71] This could also explain the observed increase in the polydispersity of HPG-*g*-PDMA/PNIPAm polymer (entries C4 and C7). Thus, all these methods offer ways to fine-tune the final structure of co-grafted mixed arm star polymer. Also, the results given in Table 2 show that only selected conditions produced controlled ATRP of NIPAM from HPG-*g*-PDMA macroinitiators.

Temperature Responsive Properties of HPG-*g*-PDMA/PNIPAm Polymers. We have utilized the temperature sensitive properties of PNIPAm to generate reversible nanoaggregates (core−shell structure) above the LCST of PNIPAm by controlling the composition and molecular weight of the PNIPAm core and PDMA corona. As hypothesized previously, longer PDMA arms could stabilize shorter PNIPAm core in the cografted mixed arm star polymer above the LCST of the PNIPAm, thus preventing precipitation from solution. At appropriate composition/molecular weight of PNIPAm and PDMA, the copolymers should form soluble nanoparticles with a reversible hydrophobic core consisting of collapsed PNIPAm chains and HPG stabilized by soluble PDMA coronas in aqueous solution above the LCST of PNIPAm.

We have measured the LCSTs of the aqueous polymer solutions at 1 mg/mL using a UV−vis spectrophotometer by monitoring the transmittance of the polymer solutions as a function of temperature at $\lambda = 500$ nm and at a heating rate of 0.5 °C/min. The transmittance values for aqueous solutions of three different co-grafted star copolymers with different PNIPAm arm lengths (entries C1, C3, and C5, Table 2) at different temperatures are shown in Figure 2. All the co-grafted mixed arm star copolymers formed clear solutions and appeared to be soluble below 35 °C. In aqueous solution the temperature dependence of the transmittance depended on polymer composition. The polymer with low PNIPAm content (HPG-*g*-PDMA(75K)/PNIPAm(2.5K) (entry C1, Table 2) produced a slightly turbid solution above 35 °C, whereas other polymers (HPG-*g*-PDMA(75K)/PNIPAm(29K) (entry C3, Table 2) and HPG-*g*-PDMA(244K)/PNIPAm(156K) entry C5, Table 2) produced a milky solution above 35 °C (Figure 2). With an increase

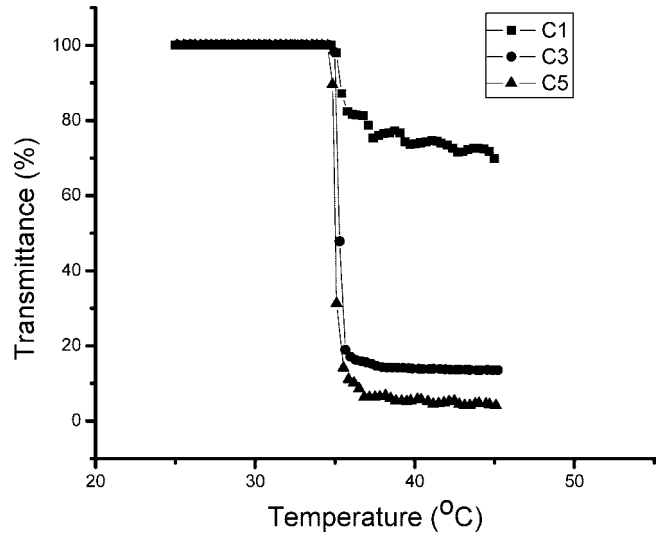

Figure 2. Transmittance curves of a 0.1 wt % aqueous solutions of three different mixed arm star copolymers (HPG-PDMA)(75K)-PNIPAm(2.5K) = C1; HPG-PDMA(75K)PNIPAm(29K) = C3; HPG-PDMA(244K)PNIPAm(156K) = C5; see Table 2) with temperature at $\lambda = 500$ nm.

in PNIPAm molecular weight or content in the cografted polymer, there is a tendency for it to aggregate more strongly and precipitate in aqueous solution above the LCST. At high PNIPAm content, the stabilizing effect of the PDMA chains is not sufficient to prevent the polymer from precipitating. The transition showed some hysteresis (∼3−4 °C) when the temperature change is reversed (data not shown), the heating curve showing a higher transition temperature than the cooling curves. A similar observation was reported previously for high molecular weight PNIPAm[72] and is believed due to chain entanglement in the aggregate above the LCST that requires higher solubility (lower temperature) to reverse at the cooling rates employed here. The increase in LCST of the star copolymers relative to the pure PNIPAm (LSCT of 32 °C[72]) is due to the presence of the co-grafted hydrophilic PDMA.

The phase transition of star copolymers was further probed using ^{1}H NMR, which provides a powerful tool for analysis of dynamic behavior of surfactant molecules in colloidal systems and the pH and temperature behavior of responsive or smart polymers.[12,73,74] Figure 3 shows ^{1}H NMR spectra of HPG-*g*-PDMA(75K)/PNIPAm(2.5K) (Table 2, entry C1) at different temperatures. The polymer sample was completely soluble at 25 °C, and the characteristic signals of PDMA and PNIPAm chains were seen on ^{1}H NMR. With increase in temperature to 35 °C, the intensity of the PNIPAm signals decreased and shifted slightly downfield, consistent with collapse of PNIPAm chains in the mixed arm star copolymer and the formation of an immobile structure. At 40 °C, the PNIPAm signal completely disappeared which showed that the PNIPAm chains are part of a quite rigid structure due to strong hydrophobic interactions. The protons from PDMA chains were still observable in the ^{1}H NMR spectra at all temperatures, however, showing that they remain in the soluble state in aqueous solution. Similar observations were made for other star copolymers (data not shown).

Laser Light Scattering Studies. LLS study gives more detailed view on the aggregation behavior of the mixed arm star copolymers. Figure 4 shows the temperature dependence of hydrodynamic radius ($\langle R_h \rangle$) of all the samples at high (0.5 mg/mL) and low (0.0625 mg/mL) concentrations. (The original data of Figure 4 are listed in Table 1S). It is worth noting that the $\langle R_h \rangle$ of C7 below 32 °C is ca. 12 nm, which is smaller than

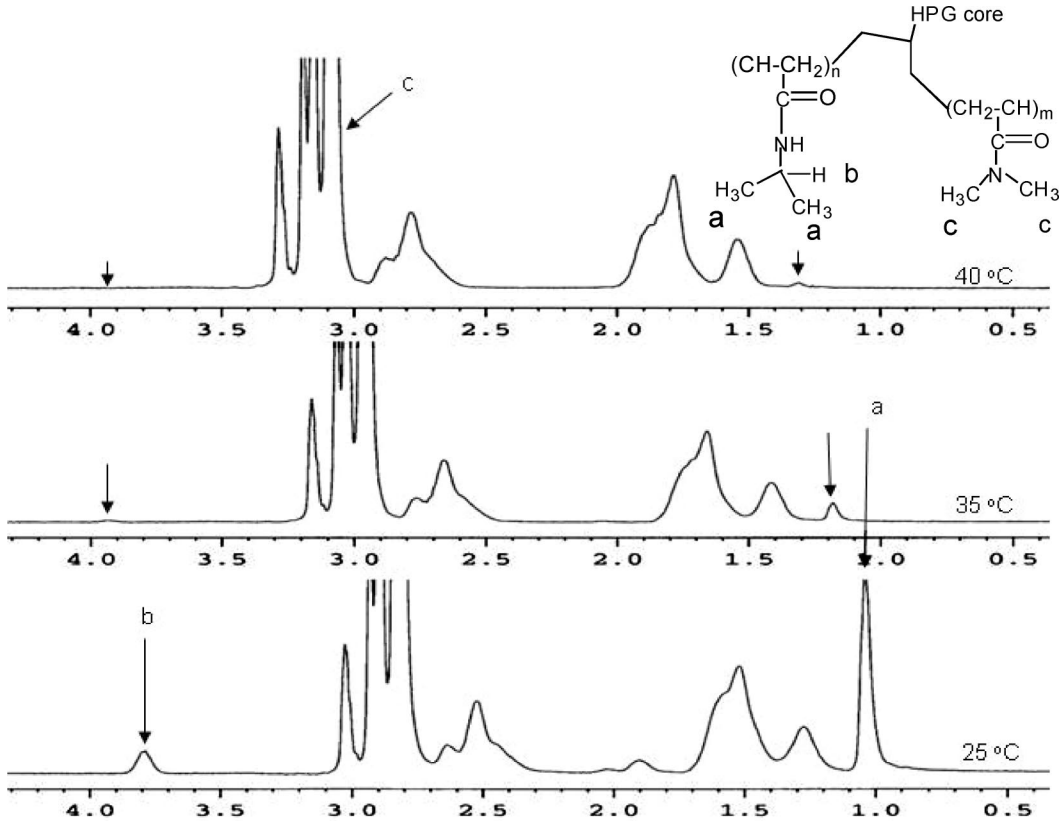

Figure 3. ^{1}H NMR spectra for mixed arm star copolymer HPG-*g*-PDMA(75K)/PNIPAm(2.5K) (C1, Table 2) in D_2O at different temperatures: (a) 25, (b) 35, and (c) 40 °C.

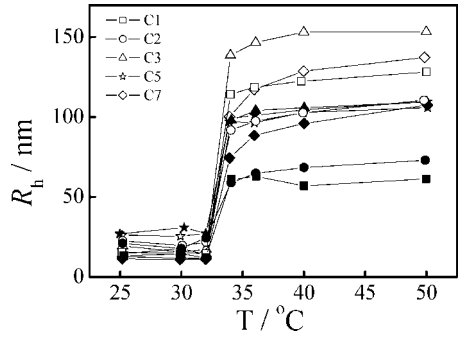

Figure 4. Temperature dependence of hydrodynamic radius of each sample at high (0.5 mg/mL, hollow) and low (0.0625 mg/mL, solid) concentrations. The suffixes of each sample denote their concentrations.

those of other samples, especially C1, C2, and C3, whose molecular weights are even smaller than C7. This should be attributed to the formation of small and stable aggregates formed even below the LCST of PNIPAm. While for the sample C7, because of its relatively long hydrophilic PDMA arms and comparably short PNIPAM arms, it has enough corona stability and thereby exists as single molecules (unimers) in water. Furthermore, when the C3 (HPG-*g*-PDMA(75K)-PNIPAm-(29K)) and C5 (HPG-*g*-PDMA(244K)-PNIPAm(156K)) were dissolved in less polar solvent methanol at room temperature, molecular dissolution was observed as evidenced by the mean hydrodynamic radius obtained by dynamic light scattering of ~13 and 17 nm, respectively, independent of concentration. In this solvent evidently the interchain association of PNIPAm was sufficiently reduced to eliminate the small aggregates found at the same temperature in water.

The most probable reason for the copolymer aggregation at low temperature is due to the intermolecular association between the relatively hydrophobic PNIPAM compared to PDMA chains. This argument is supported by the measured $\langle R_h \rangle$ of the mixed star polymers at different compositions at 25 °C. The mixed star polymers with high PNIPAM content (C2, C3, C5) relative to PDMA has shown more aggregation (large $\langle R_h \rangle$) than with low PNIPAM content (C1, C7) (Table 2S, Supporting Information). At higher PNIPAM content (i.e., increase in chain length of PNIPAM), the PNIPAM may be getting more exposed to water. Another plausible reason for the observed large hydrodynamic size of the polymer is the possibility of few percentages of interconnected star polymers in our samples. Our initial light scattering experiments showed the presence of a little amount of large particles in C1, C2, C3, and C5 and not in C7; so we have used 100 nm filter (see Experimental Section) to remove them. We have taken every care to remove large aggregates before the light scattering measurements. But this procedure may not have removed all of the large particles from the sample. Further analyses of light scattering data (weight distribution analysis) have shown that there is a possibility of presence of star−star coupled product in the final polymer samples. The results show that samples C1, C2, and C3 may have ~0.2,~0.5, and ~2.0 weight fraction of star−star coupled product, respectively, and the sample C5 has a higher percentage of star−star coupled product (~25 weight fraction). This may be contributing to the large $\langle R_h \rangle$ values at low temperatures for C5. Another reason for the observed higher hydrodynamic size of the mixed star copolymers is due to the hydrophobic interactions between the molecules due to the presence of relatively higher hydrophobicity of PNIPAM compared to PDMA. This argument is based on the absence of very high molecular weight polymer molecules in the samples as seen from the GPC-MALLS data (Figures 10S−17S in Supporting Information). Since the LLS measurements were done under static conditions unlike flow conditions in GPC-MALLS (loose aggregates can easily be broken down to individual molecules under these shear condi-

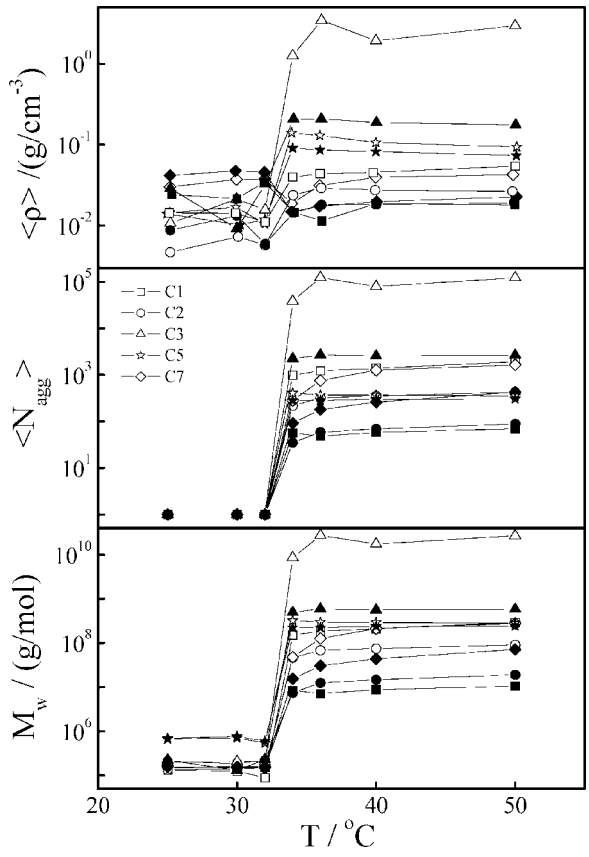

Figure 5. Temperature dependence of weight average molar mass (M_w), average aggregation number ($\langle N_{agg}\rangle$), and average density ($\langle\rho\rangle$) (hollow symbol, 0.5 mg/mL; solid symbol, 0.0625 mg/mL).

tions), we attribute presence of species with large hydrodynamic size in sample C5 is due to the aggregation of HPG-*g*-PDMA/PNIAM molecules via hydrophobic interaction.

The relatively insensitive nature of phase transition temperature on the molecular weight and composition of star polymer is due to the high molecular weight of the star polymers and co-grafted nature of PNIPAM chains (Figure 4). Unlike the conventional stimuli responsive copolymers, in the present case the property of the PNIPAM chains may not influenced by the adjacent monomer structure (Figure 1). The $\langle R_h\rangle$ of the star copolymers increase sharply at 32 °C at both concentrations and then slowly increase as the temperature increases from 34 to 50 °C. For a given star copolymer, the aggregation size increases with concentration, implying micelle-like behavior. Furthermore, from the SLS measurement, the radius of gyration ($\langle R_g\rangle$) of aggregates at different temperature and concentrations can be obtained (listed in Table 2S). As is well-known, the ratio of $\langle R_g\rangle/\langle R_h\rangle$ are 0.774 for a uniform solid sphere and 0.45 for a micelle-like structure with compact core, respectively.[75,76] In our experiment, $\langle R_g\rangle/\langle R_h\rangle$ values of all the samples are in the range of 0.5−0.6 except C3, which further indicates that the resulted aggregates have micelle-like structures.

Figure 5 shows the temperature dependence of weight-average molar mass (M_w), average aggregation number ($\langle N_{agg}\rangle$), and average density (ρ), where $\langle N_{agg}\rangle$ and $\langle\rho\rangle$ are defined as $M_{w,T}/M_{w,25\ °C}$ and $M_w/[(4/3)\pi\langle R_h\rangle^3]$, respectively. Note that in Figures 4 and 5, compared with the samples with higher PNIPAM content (C3 and C5), copolymers with relatively low PNIPAM content (C1, C2, and C7) generally have smaller $\langle R_h\rangle$, $\langle\rho\rangle$, $\langle N_{agg}\rangle$, and M_w. Furthermore, it is interesting to notice that sample C5 shows relatively lower aggregation number at higher concentration, which could be attributed to the high content of hydrophilic PDMA. The long soluble PDMA chains possess the maximum stabilization effect, and they also could prevent the further aggregation because of the steric hindrance, which could also account for the largest values of $\langle R_h\rangle$, M_w, $\langle N_{agg}\rangle$, and $\langle\rho\rangle$ for C3 among all the samples, although it has lower PNIPAM content than C5. The effect of PDMA chains can be better viewed by comparing the chain density before and after aggregation. It is easy to imagine that the shrinking of the PNIPAM arms will make the chain density increase, but on the contrary, we notice that for C1, C2, and C7 the chain density changed slightly, which could be due to the covalent attachment of arms on a less flexible hyperbranched core compared to a linear polymer.[77] The difference in the behavior of C3 and C5 compared to C1, C2, and C7 could be due to the higher molecular weight of PNIPAm arms (higher PNIPAM content) relative to PDMA arms (Table 2). The change in chain density, before and after aggregation, also indicates the relative loose structures of the resulting aggregates.

We were able to draw a more complete picture of the assembly of these polymers by looking at the data in the whole temperature range investigated. In the beginning, even when temperature is low, the copolymers exist as small aggregates in water, except C7, which has enough corona stability of long PDMA chain. As the temperature increased above 32 °C, the PNIPAm chains in the star copolymers collapsed and the stabilization effect of the hydrophilic PDMA corona of the single molecule or small aggregate was not sufficient to stabilize its hydrophobic core. So the cores are prone to aggregate under the hydrophobic interaction and force the hydrophilic PDMA chains in the aggregate to remain outside to form the hydrophilic corona and form aggregates with relatively loose and uniform micelle-like structure. The molecular weight of PDMA arms and the relative PDMA/PNIPAm content play important roles in this process. Our light scattering results show that none of the polymers synthesized form unimolecular micelle structures as expected but rather formed small aggregates with stabilized PDMA corona.

Conclusions

A multi-initiator-functionalized hyperbranched polyglycerol was synthesized. Well-defined mixed arm star copolymers of thermoresponsive (PNIPAm) and non-thermoresponsive (PDMA) were synthesized by sequential of RAFT and ATRP techniques by a two-step polymerization method. Controlled RAFT polymerization of *N,N*-dimethylacrylamide was achieved using *S,S′*-bis(α,α′-dimethyl-α″-acetic acid)trithiocarbonate as chain transfer agent in acetic acid/sodium acetate buffer. The ratio of [CTA]/[azo initiator] was critical in controlling the molecular weight and polydispersity of the HPG-*g*-PDMA copolymers. Co-grafted star copolymers containing PNIPAm were synthesized by a subsequent ATRP of *N*-isopropylacrylamide from HPG-*g*-PDMA macroinitiators in aqueous solutions. The molecular weight of the star copolymer was manipulated by changing the catalyst and monomer concentration and HPG-*g*-PDMA macroinitiator molecular weight. The new star copolymers showed LCST values around 35 °C. Temperature-dependent dynamic and static light scattering studies showed that the mixed arm star copolymers exist either as individual molecules or as intermolecular aggregates below the phase transition temperature of PNIPAm. With increase in temperature above the LCST (>32 °C), the thermoresposive PNIPAm arms in the star copolymer collapsed to form a hydrophobic core which was stabilized by soluble PDMA arms. The LLS studies showed that all the star copolymers form intermolecular aggregates above the LSCT through possible hydrophobic interactions between the collapsed PNIPAm chains and the aggregates are stabilized by the PDMA corona. It was found that the aggregation or stabilization of core−corona structure

depends on the molecular weight of the arms and PNIPAm/PDMA content. The ratio of $\langle R_g \rangle / \langle R_h \rangle$ suggests that the aggregates have micelle-like structure.

Acknowledgment. We thank the Centre for Blood Research, Canadian Institutes of Health Research, Canadian Blood Services (CBS), Canada Foundation of Innovation, and Michael Smith Foundation for Health Research for financial support. J.N.K. is the recipient of a CBS/CIHR new investigator award in transfusion science. K.R. acknowledges a postdoctoral fellowship from the Strategic Training Program in Transfusion Science at the Centre for Blood Research supported by CIHR and Heart and Stroke Foundation of Canada.

Supporting Information Available: Additional figures of GPC traces, cumulative weight fraction vs molar mass figures of HPG-*g*-PDMA and HPG-*g*-PDMA/PNIPAm, and a table containing R_g and R_h values. This material is available free of charge via the Internet at http://pubs.acs.org.

References and Notes

(1) Sun, T.; Wang, G.; Feng, L.; Liu, B.; Ma, Y.; Jiang, L.; Zhu, D. *Angew. Chem., Int. Ed.* **2004**, *43*, 357.
(2) (a) Zhao, B.; Brittain, W. J.; Zhou, W.; Cheng, S. Z.; D, *J. Am. Chem. Soc.* **2000**, *122*, 2407. (b) Kizhakkedathu, J. N.; Norris-Jones, R.; Brooks, D. E. *Macromolecules* **2004**, *37*, 734.
(3) Collier, J. H.; Messersmith, P. B. *Adv. Mater.* **2004**, *16*, 907.
(4) Bellomo, E. G.; Wyrsta, M. D.; Pakstis, L.; Pochan, D. J.; Deming, T. J. *Nat. Mater.* **2004**, *3*, 244.
(5) Chen, G. H.; Hoffman, A. S. *Nature (London)* **1995**, *373*, 49.
(6) Yamazaki, A.; Song, J. M.; Winnik, F. M.; Brash, J. L. *Macromolecules* **1998**, *31*, 109.
(7) Colfen, H. *Macromol. Rapid Commun.* **2001**, *22*, 219.
(8) Lutz, J.-F.; Akdemir, O.; Hoth, A. *J. Am. Chem. Soc.* **2006**, *128*, 13046.
(9) Idziak, I.; Avoce, D.; Lessard, D.; Gravel, D.; Zhu, X. X. *Macromolecules* **1999**, *32*, 1260.
(10) Yamazaki, A.; Song, J. M.; Winnik, F. M.; Brash, J. L. *Macromolecules* **1998**, *31*, 109.
(11) Butun, V.; Billingham, N. C.; Armes, S. P. *Chem. Commun.* **1997**, 671.
(12) Vamvakaki, M.; Palioura, D.; Spyros, A.; Armes, S. P.; Anastasiadis, S. H. *Macromolecules* **2006**, *39*, 5106.
(13) Amalvy, J. I.; Wanless, E. J.; Li, Y.; Michailidou, V.; Armes, S. P. *Langmuir* **2004**, *20*, 8992.
(14) Zhao, X.; Zhang, Z.; Pan, F.; Ma, Y.; Armes, S. P.; Lewis, A. L.; Lu, J. R. *Langmuir* **2005**, *21*, 9597.
(15) Wan, D.; Fu, Q.; Huang, J. *J. Polym. Chem., Part A: Polym. Chem.* **2005**, *43*, 5652.
(16) Porjazoska, A.; Dimitrov, P.; Dimitrov, I.; Cvetkovska, M.; Tsvetanov, C. B. *Macromol. Symp.* **2004**, *210*, 427.
(17) Kujawa, P.; Tanaka, F.; Winnik, F. M. *Macromolecules* **2006**, *39*, 3048.
(18) Xia, Y.; Yin, X.; Burke, N. A. D.; Stover, H. D. H. *Macromolecules* **2005**, *38*, 5937.
(19) Riess, G. *Prog. Polym. Sci.* **2003**, *28*, 1107, and references therein.
(20) Nedelcheva, A. N.; Vladimirov, N. G.; Novakov, C. P.; Berlinova, I. V. *J. Polym. Sci., Part A: Polym. Chem.* **2004**, *42*, 5736.
(21) Zhang, S.; Qing, J.; Xiong, C.; Peng, Y. *J. Polym. Sci., Part A: Polym. Chem.* **2004**, *42*, 3527.
(22) Liu, B.; Perrier, S. *J. Polym. Sci., Part A: Polym. Chem.* **2005**, *43*, 3643.
(23) Pispas, S. *J. Polym. Sci., Part A: Polym. Chem.* **2005**, *44*, 606.
(24) Lee, A. S.; Gast, A. P.; Bütün, V.; Armes, S. P. *Macromolecules* **1999**, *32*, 4302.
(25) Li, Y.; Armes, S. P.; Jin, X.; Zhu, S. *Macromolecules* **2003**, *36*, 8268.
(26) Ma, Y.; Tang, Y.; Billingham, N. C.; Armes, S. P.; Lewis, A. L.; Lloyd, A. W.; Salvage, J. P. *Macromolecules* **2003**, *36*, 3475.
(27) Liu, S.; Armes, S. P. *Angew. Chem., Int. Ed.* **2002**, *41*, 1413.
(28) Liu, S.; Billingham, N. C.; Armes, S. P. *Angew. Chem., Int. Ed.* **2001**, *40*, 2328.
(29) André, X.; Zhang, M.; Müller, A. H. E. *Macromol. Rapid Commun.* **2005**, *26*, 558.
(30) Solomatin, S. V.; Bronich, T. K.; Eisenberg, A.; Kabanov, V. A.; Kabanov, A. V. *Langmuir* **2004**, *20*, 2066.
(31) Agut, W.; Brulet, A.; Taton, D.; Lecommandoux, S. *Langmuir* **2007**, *23*, 11526–11533.
(32) Gotzamanis, G.; Tsitsilianis, C. *Polymer* **2007**, *48*, 6226–6233.
(33) Ge, Z.; Xie, D.; Chen, D.; Jiang, X.; Zhang, Y.; Liu, H.; Liu, S. *Macromolecules* **2007**, *40*, 3538–3546.
(34) Xu, J.; Ge, Z.; Zhu, Z.; Luo, S.; Liu, H.; Liu, S. *Macromolecules* **2006**, *39*, 8178–8185.
(35) Mountrichas, G.; Pispas, S. *Macromolecules* **2006**, *39*, 4767–4774.
(36) Ge, Z.; Cai, Y.; Yin, J.; Zhu, Z.; Rao, J.; Liu, S. *Langmuir* **2007**, *23*, 1114–1122.
(37) Lambeth, R,H.; Ramakrishnan, S.; Mueller, R.; Poziemski, J. P.; Miguel, G. S.; Markoski, L. J.; Zukoski, C. F.; Moore, J. S. *Langmuir* **2006**, *22*, 6352–6360.
(38) Lupitskyy, R.; Roiter, Y.; Tsitsilianis, C.; Minko, S. *Langmuir* **2005**, *21*, 8591–8593.
(39) Gitsov, I.; Frechet, J. M. J. *J. Am. Chem. Soc.* **1996**, *118*, 3785–6.
(40) Liu, C.; Zhang, Y.; Huang, J. *Macromolecules* **2008**, *41*, 325–331.
(41) Mountrichas, G.; Mpiri, M.; Pispas, S. *Macromolecules* **2005**, *38*, 940.
(42) Lele, B. S.; Leroux, J.-C. *Polymer* **2002**, *43*, 5595.
(43) Narrainen, A. P.; Pascual, S.; Haddleton, D. M. *J. Polym. Sci., Part A: Polym. Chem.* **2002**, *40*, 439.
(44) Nakashima, K.; Bahadur, P. *Adv. Colloid Interface Sci.* **2006**, *123−126*, 75000.
(45) Pispas, S.; Poulos, Y.; Hadjichristidis, N. *Macromolecules* **1998**, *31*, 4177.
(46) Yoo, M.; Heise, A.; Hedrick, J. L.; Miller, R. D.; Frank, C. W. *Macromolecules* **2003**, *36*, 268.
(47) Xu, J.; Luo, S.; Shi, W.; Liu, S. *Langmuir* **2006**, *22*, 989.
(48) Wang, J.; Matyjaszewski, M. *J. Am. Chem. Soc.* **1995**, *117*, 5614.
(49) Matyjaszewski, K.; Xia, J. *Chem. Rev.* **2001**, *101*, 2921.
(50) Kamigaito, M.; Ando, T.; Sawamoto, M. *Chem. Rev.* **2001**, *101*, 3689.
(51) Chiefari, J.; Chong, Y. K.; Ercole, F.; Krstina, J.; Jeffery, J.; Le, T. P. T.; Mayadunne, R T. A.; Meijs, G. F.; Moad, C. L.; Moad, G.; Rizzardo, E.; Thang, S. H. *Macromolecules* **1998**, *31*, 5559.
(52) (a) McCormick, C. L.; Lowe, A. B. *Acc. Chem. Res.* **2004**, *37*, 312. (b) Moad, G.; Rizzardo, E.; Thang, S. H. *Aust. J. Chem.* **2005**, *58*, 379–410.
(53) (a) Venkatesh, R.; Yajjou, L.; Koning, C. E.; Klumperman, B. *Macromol. Chem. Phys.* **2004**, *205*, 2161–2168. (b) Cheng, Z.; Zhu, X.; Fu, G. D.; Kang, E. T.; Neoh, K. G. *Macromolecules* **2005**, *38*, 7187–7192.
(54) Ciampolini, M.; Nardi, N. *Inorg. Chem.* **1966**, *5*, 41.
(55) Lai, J. T.; Filla, D.; Shea, D. *Macromolecules* **2002**, *35*, 6754.
(56) Kizhakkedathu, J. N.; Rajesh Kumar, K.; Goodman, D.; Brooks, D. E. *Polymer* **2004**, *45*, 7471.
(57) Sunder, A.; Hanselmann, H.; Frey, H.; Mulhaupt, R. *Macromolecules* **1999**, *32*, 4240.
(58) Salazar, R.; Fomina, L.; Fomine, S. *Polym. Bull.* **2001**, *47*, 151.
(59) Rajesh Kumar, K.; Kizhakkedathu, J. N.; Brooks, D. E. *Macromol. Chem. Phys.* **2004**, *205*, 567.
(60) Taton, D.; Wilczewska, A. Z.; Destarac, M. *Macromol. Rapid Commun.* **2001**, *22*, 1497.
(61) Benaglia, M.; Rizzardo, E.; Alberti, A.; Guerra, M. *Macromolecules* **2005**, *38*, 3129.
(62) Donovan, M. S.; Sanford, T. A.; Lowe, A. B.; Sumerlin, B. S.; Mitsukami, Y.; McCormick, C. L. *Macromolecules* **2002**, *35*, 4570.
(63) Baussard, J.-F.; Habib-Jiwan, J.-L.; Laschewsky, A.; Mertoglu, M.; Storsberg, J. *Polymer* **2004**, *45*, 3615.
(64) Thomas, D. B.; Convertine, A. J.; Hester, R. D.; Lowe, A. B.; McCormick, C. L. *Macromolecules* **2004**, *37*, 1735.
(65) Kizhakkedathu, J. N.; Brooks, D. E. *Marcomolecules* **2003**, *36*, 591.
(66) Perrier, S.; Takolpuckdee, P.; Mars, C. A. *Macromolecules* **2005**, *38*, 2033.
(67) (a) Chen, Y.; Shen, Z.; Barriau, E.; Kautz, H.; Frey, H. *Biomacromolecules* **2006**, *7*, 919. (b) Shen, Z.; Chen, Y.; Barriau, E.; Frey, H. *Macromol. Chem. Phys.* **2006**, *207*, 57.
(68) Angot, S.; Murthy, K. S.; Taton, D.; Gnanou, Y. *Macromolecules* **1998**, *31*, 7218–7225.
(69) (a) Percec, V.; Guliashvili, T.; Ladislaw, J. S.; Wistrand, A.; Stjerndahl, A.; Sienkowska, M. J.; Monterio, M. J.; Sahoo, S. *J. Am. Chem. Soc.* **2006**, *128*, 141–14165. (b) Percec, V.; Popov, A. V.; Ramirez-Castillo, E.; Monterio, M. J.; Barboiu, B.; Weichold, O.; Asandei, A.d.; Mitchell, C. M. *J. Am. Chem. Soc.* **2002**, *124*, 4940–4941.
(70) Matyjaszewski, K.; Patten, T. E.; Xia, J. *J. Am. Chem. Soc.* **1997**, *119*, 674–680.
(71) Teodorescu, M.; Matyjaszewski, K. *Macromolecules* **1999**, *32*, 4826–4831.
(72) Gao, J.; Wu, C. *Macromolecules* **1997**, *30*, 6873–6876.
(73) Kriz, J.; Masar, B.; Pospisil, H.; Plestil, J.; Tuzar, Z.; Kiselev, M. A. *Macromolecules* **1996**, *29*, 7853.
(74) Liu, B.; Perrier, S. *J. Polym. Chem., Part A: Polym. Chem.* **2005**, *43*, 3643.
(75) Burchard, W.; Schmidt, M.; Stockmayer, W. H. *Macromolecules* **1980**, *13*, 1265–1272.
(76) Acksasu, A. Z.; Han, C. C. *Macromolecules* **1979**, *12*, 276–280.
(77) Qiu, X.; Wu, C. *Macromolecules* **1997**, *30*, 7921–7926.

MA800094D